



Precipitable Water Vapour Retrieval Modelling Using Indian Regional Navigation Satellite System (IRNSS) Observations over Dehradun

Ashutosh Srivastava

Indian Institute of Remote Sensing, Dehradun, Uttarakhand 248 001, India

Received 1 January 2024; accepted 6 November 2024

In the present work, a maiden attempt has been made to derive precipitable water vapour (PWV) using IRNSS datasets. A least square differential correction approach is used in modelling to process datasets. PWV is estimated for different days of January, April, July, and November of the year 2019 to observe its variation over different seasons. Meteorological datasets used in the estimation of zenith hydrostatic delay (ZHD) and weighted mean temperature estimation are taken from the National Centers for Environmental Prediction (NCEP) at the location. The obtained PWV values are validated with GPS-derived PWV and Modern-Era Retrospective Analysis for Research and Applications (MERRA) reanalysis datasets. The results show that PWV derived using IRNSS datasets are close to the other reference values. The difference of 3 mm to 7 mm was observed if compared with GPS-derived PWV and MERRA PWV values. Since each satellite signal is available at all times, PWV is estimated using the individual satellite data and combined data from all the IRNSS satellites. As the IRNSS constellation includes both geostationary and geosynchronous satellites, it is observed that PWV estimated using geostationary satellite datasets is close to the reference datasets having a difference of 3 to 5 mm. However, estimated PWV using geosynchronous satellite data have more variation with differences within 3 to 7 mm. Combined data from all the satellites was also used to derive the PWV which has a difference of close to 5 mm in all the cases. The obtained PWV values using IRNSS data show a good correlation with GPS PWV and MERRA PWV values and provide a good estimate of PWV.

Keywords: Precipitable water vapour; Zenith hydrostatic delay; Global positioning systems

1 Introduction

The primary objective of navigation constellations is to provide precise positions at various levels. Ground or space-based receivers receive the signals from these satellites which are used to find their position. Various constellations are available in space. Global positioning systems (GPS) owned by the United States of America, GALILEO by the European space agency, Russia's GLONASS, and BeiDou from China are a few examples of such constellations. India also developed its navigation constellation named Indian Regional Navigation Satellite System (IRNSS) also called Navigation with Indian Constellation (NavIC), to provide services within the Indian region. The seven-satellite constellation, IRNSS developed by the Indian Space Research Organization (ISRO) is designed to provide precise positions to the users in the primary service area (India and 1500 km around the Indian mainland). Though these constellations are primarily used for precise positioning, their signals also can be used to derive atmospheric parameters as

they travel from the satellite to the receiver and carry the atmospheric information.

Precipitable water vapour is such a parameter that is important for various atmospheric analyses like weather forecasting, nowcasting, rainfall prediction, weather monitoring, *etc.* Precipitable water vapour not only affects the troposphere area but is also a noticeable source of water in the stratospheric area. It is a common and more efficient greenhouse gas than carbon dioxide, primarily for global warming. The water vapour passes the short-wave radiation coming from the sun but traps the longwave radiation going back from the Earth's atmosphere and thus the temperature will rise and also the water vapour will rise which increases the greenhouse effect. The water vapour also plays a continuity during the condensation process and the process of vapour formation. The most important thing is that until today water vapour estimation and monitoring using various techniques is still limited. On the other side, global navigation satellite system (GNSS)-based PWV retrieval is the new dimension that provides continuous measurements, unlike other ground and space-based measurements

*Corresponding author: (E-mail: drsrivastava82@gmail.com)

which have spatiotemporal limitations or are not cost effective. In the process of PWV retrieval, zenith tropospheric delay (ZTD) is estimated after processing GNSS data which is further used for zenith wet delay estimation (ZWD) after subtraction of zenith hydrostatic delay (ZHD). This ZWD is further used in PWV computation.

Various studies have been made for PWV retrieval using GNSS data and its impact on the atmosphere. Bevis *et al.* gave a concept of GNSS meteorology and stated that dense Global Positioning System (GPS) networks could be used to derive the vertical distribution of water vapour in the local area¹. Niell presented global mapping functions to estimate delay in radio signals at different elevation angles². Dai *et al.* derived PWV from using 54 North American GPS stations data and studied its diurnal variations for the period 1996–2000³. Wang *et al.* developed an analysis technique to convert ZPD to PWV on a global scale and produced a 2 hourly PWV dataset from ground-based GPS measurements⁴. Jade and Vijayan first time used the Indian GNSS network data and derived PWV using GPS and NCEP reanalysis data over the region⁵. Adams *et al.* proposed the world's first equatorial GNSS meteorology network to examine the evolution of water vapour during the shallow-to-deep convection transition, mesoscale organization, and propagation of convective systems in the Amazon Region⁶. Bonafoni *et al.* assessed the accuracy of PWV from the GPS network in central Italy as around 0.07 cm⁷. Joshi *et al.* derived the PWV for the central Himalayan district and compared it with MODIS data⁸. Shoji *et al.* estimated PWV around CORS at the local level using slant path delay⁹. Arboledas *et al.* evaluated the AERONET water vapour and compared it with GPS, radiosonde, and microwave radiometry measurements¹⁰. Singh *et al.* estimated the precipitable water vapour from GPS-derived zenith delays using radiosonde data in India¹¹. Alshawaf *et al.* estimated the atmospheric water vapour using GNSS and surface meteorological data and compared it with the WRF produced PWV, which shows a good agreement with GNSS-derived PWV¹². Liang *et al.* used the Chinese GNSS network data for precipitable water vapour measurements and its meteorological applications¹³. Lu *et al.* used the Beidou and GPS data for real time precipitable water vapour retrieval and produced comparable results¹⁴. Jiang estimated PWV using GNSS data over China and carried out a comparative study with the NWP reanalysis and Sun photometer data sets¹⁵. Isioye *et al.*

carried out a study on GNSS-based PWV estimation over Nigeria¹⁶. The obtained results are compared with AIRS and reanalysis datasets. Kitpracha *et al.* estimated precise tropospheric delay using the GNSS PPP technique in Thailand and compared the results with IGS products and tropospheric model results¹⁷. Hankansujarit and Andrei processed the CUSV IGS station data using the PPP method for PWV derivation¹⁸. Yao *et al.* proposed a fusion model for the integration of GNSS and ECMWF data PWV data for accuracy improvement¹⁹. Zhang *et al.* have retrieved the precipitable water vapour using ground and space-based GNSS, Radiosonde, microwave satellite, and NWP reanalysis data and conducted a comparative analysis among all²⁰. Recently, Liu *et al.* used an interpolation method for refining the precipitable water vapour (PWV) values derived from GNSS. They have shown that the predicted performance of the new method is better than the conventional method²¹. Meunram and Satirapod derived the PWV over Thailand and carried out an analysis to determine the PWV coverage distance from each CORS and found that PWV derived from CORS will be useful within the radius of 74 km from CORS²². Darrag *et al.* estimated the PWV for the east Mediterranean using GNSS and observed the highest temporal and spatial variation values were 25.41 mm and 19.67 mm, respectively²³.

In most of these studies, GPS data are used primarily which is the medium earth orbit (MEO) constellation. In this work, for the first time a study has been made to derive precipitable water vapour using IRNSS datasets which are also GEO based constellation. Though the IRNSS is used for precise positioning primarily, the satellite data received by a ground-based receiver also can be used for atmospheric applications like other constellations. An IRNSS receiver developed by “Accord Software and Systems” is set up at the Indian Institute of Remote Sensing (IIRS), Dehradun in static mode (Fig. 1). This continuously operating receiver receives the signals from all satellites of the IRNSS constellation, processes the datasets, converts it into readable formats, and provides accurate positioning. IRNSS datasets from this receiver are retrieved and used for PWV estimation. PWV is estimated for the various days of different months in a year to observe its variation over the months. PWV is computed using the data of individual satellites to observe the PWV results separately. However, PWV is also estimated using combined data from different sources, since it



Fig. 1 — IRNSS (NaVIC) receiver

covers different directions and angular heights. The obtained results are very well compared with the GPS-derived PWV results and MERRA2 reanalysis data. Finally, a detailed statistical analysis is made to compare and validate the obtained results.

2 Data Description and Methodology

IRNSS has seven satellites in its constellation, out of seven four are geosynchronous satellites located at 2 each at 55° and 111° longitudes and three are geostationary satellites which are located at 34.5°, 83° and, 131.5° longitudes. The elevation angles for two geosynchronous satellites are 29° and for the other two are -29°. IRNSS receiver provides L5 data at a 1-sec interval which are taken in the present study. Raw datasets are processed through the software which is provided by Accord Software and Systems. The processed data contain pseudoranges, receiver position, IRNSS satellite orbital parameters, ionospheric delay, and receiver and satellite clock corrections which are downloaded in MS Excel format. Ionospheric delay can be estimated using either Klobuchar, grid-based, or dual frequency models as provided in the IRNSS ICD document²⁴. However, to estimate the PWV over a particular region, a more precise tropospheric delay is required which is obtained using IRNSS data in the present study. A detailed methodology adopted to estimate PWV using IRNSS data is discussed in the following sub-sections.

2.1 Tropospheric delay estimation

The receiver receives the signal at a time t_1 which was transmitted from the IRNSS satellite at time t . The pseudorange (P) is estimated by multiplying the velocity of light in time difference.

$$P = c * \Delta t, \text{ where } \Delta t = t_1 - t \text{ and } c \text{ is the speed of light} \quad \dots (1)$$

This pseudorange includes the information of a tropospheric delay, ionospheric delay, receiver and satellite clock errors along with the geometric range as given in Eq. (2).

$$P = \rho + c * \delta_t - c * \delta^{t_1} + T + I + M + e \quad \dots (2)$$

Where ρ is the geometric distance between the satellite and the receiver, δ_t is the receiver clock error, δ^{t_1} is the satellite clock error, T path delay due to troposphere and I is the delay because of the Ionosphere. M is the multipath delay and depends upon the receiver location. In the present case, since the receiver is placed at such a location where no obstruction takes place, M is considered zero. Pseudorange, clock errors and Ionospheric errors outputs are also taken from the processed datasets. e is the error term which includes the random error and an error that depends on elevation. Since the receiver receives the signal from the geostationary satellites which come at almost the same elevation angle and azimuths. There are very minor changes in angles in the case of geosynchronous satellites. So other than the known errors, any additional error in these directions can be fixed and modelled easily. These errors are modelled as a function of elevation and clubbed with random error e .

The geometric range between satellite and receiver is estimated using the following equation:

$$\rho = \sqrt{(x^i - x)^2 + (y^i - y)^2 + (z^i - z)^2} \quad \dots (3)$$

here, (x^i, y^i, z^i) and (x, y, z) are the coordinates of satellites and receiver respectively. $i=1,2, \dots, 7$. To obtain the zenith tropospheric delay from the IRNSS data a differential correction approach using least square estimation is adopted. A differential correction approach is an iterative method in which a continuous updation of result will be there using the new datasets in every iteration until a required result will be obtained or obtained results comes closer to predetermined threshold values. Assuming initial coordinates of the receiver is (x, y, z) and tropospheric delay is T . This initial

information about the coordinates and delay either can be taken from the receiver data or other reliable source with proper validation. If the initial guess is not correct or it is far away from the actual coordinates, then a good solution may not be obtained or it may require more iteration to get good convergence. The actual coordinates of the receiver are given as

$$x_j = x + \Delta x_j, y_j = y + \Delta y_j, z_j = z + \Delta z_j \quad \dots (4)$$

where $(\Delta x_j, \Delta y_j, \Delta z_j)$ are the deviations from the actual values and are to be included in initial values after every iteration. The actual values can be written as

$$f(x_j, y_j, z_j) = f(x + \Delta x_j, y + \Delta y_j, z_j = z + \Delta z_j) \quad \dots (5)$$

Using Taylor series $f(x + \Delta x_j, y + \Delta y_j, z_j = z + \Delta z_j)$ can be expanded as

$$f(x_j, y_j, z_j) = f(x, y, z) + \frac{\partial f(x,y,z)}{\partial x} \Delta x + \frac{\partial f(x,y,z)}{\partial y} \Delta y + \frac{\partial f(x,y,z)}{\partial z} \Delta z + \frac{1}{2!} \frac{\partial^2 f}{\partial x^2} + \dots (6)$$

The higher-order terms are neglected after the linear relation as the value of the power of small quantity will be very small further. The equation of pseudorange equation then becomes:

$$P_j = \rho_j + \frac{\partial f_j(x,y,z)}{\partial x} \Delta x + \frac{\partial f_j(x,y,z)}{\partial y} \Delta y + \frac{\partial f_j(x,y,z)}{\partial z} \Delta z + c * \Delta T \quad \dots (7)$$

In matrix presentation it can be written as:

$$\begin{bmatrix} \frac{\partial f_1}{\partial x} & \frac{\partial f_1}{\partial y} & \frac{\partial f_1}{\partial z} & \dots \\ \frac{\partial f_2}{\partial x} & \frac{\partial f_2}{\partial y} & \frac{\partial f_2}{\partial z} & \dots \\ \frac{\partial f_3}{\partial x} & \frac{\partial f_3}{\partial y} & \frac{\partial f_3}{\partial z} & \dots \\ \dots & \dots & \dots & \dots \\ \frac{\partial f_N}{\partial x} & \frac{\partial f_N}{\partial y} & \frac{\partial f_N}{\partial z} & \dots \end{bmatrix} \begin{bmatrix} \Delta x_j \\ \Delta y_j \\ \Delta z_j \\ \dots \end{bmatrix} = \begin{bmatrix} P_1 - \rho_1 \\ P_2 - \rho_2 \\ P_3 - \rho_3 \\ \dots \\ P_N - \rho_N \end{bmatrix} \quad \dots (8)$$

where N is the total no. of observations and $j=1,2,..n$ no of iterations. The Eq. (8) can be represented as

$$AX = Y \quad \dots (9)$$

A is the design matrix with $N \times 4$ dimensions. Using least square method the solution of Eq. (9) can be obtained as

$$X = (A^T A)^{-1} A^T Y \quad \dots (10)$$

which provides the values of $(\Delta x, \Delta y, \Delta z, \Delta T)$ iteratively. The receiver coordinates and tropospheric delay are updated after every iteration until convergence achieved or for fixed iterations.

2.2 Zenith tropospheric delay modelling

The IRNSS receiver receives the signals at different elevation angles from different satellites. The troposphere causes the delay in the signal's path with variable time length with respect to elevation angles. At lower elevation angles, the tropospheric delay will be maximum, while at zenith it will be minimum. To derive the PWV from IRNSS data at the receiver location, information about zenith tropospheric delay is required which can be converted from slant tropospheric delay using mapping functions. This delay is categorized in two components, hydrostatic delay and wet delay. The hydrostatic delay is estimated using the surface pressure which is almost 90% of total delay and wet delay is estimated by subtracting the hydrostatic delay from total delay. The hydrostatic delay component is present because of aerosols, gas particles, etc. On the other side, wet delay is occurred because of moisture present in the atmosphere, has less portion in the total delay, and difficult to estimate. The slant total delay at different angles can be written using Eq. (11)

$$total\ delay = ZHD * m_h(el) + ZWD * m_w(el) \quad \dots (11)$$

where ZHD is the zenith hydrostatic delay and ZWD is the zenith wet delay. $m_h(el)$ and $m_w(el)$ are the hydrostatic and wet mapping functions that are required to estimate delay at different elevation angles. Mapping functions are useful to convert the zenith delay to slant delay. There are different mapping functions which are used to derive the slant delay from the hydrostatic delay and the wet delay. In this study, Niell mapping functions are used to determine the slant tropospheric delay at different angles. The lower elevation angle datasets are not used because of more interference in the signals. ZHD is estimated using the Saastamoinen model.

$$ZHD = \frac{0.002277 * P}{1 - 0.00266 * \cos(2\phi) - 0.0028 * H} \quad \dots (12)$$

where P is the surface pressure (hPa), ϕ is the receiver latitude and H is the height of the station (Km).

The hydrostatic and wet mapping functions given in Eq. (11), is defined as

$$m_h(el) = \frac{1 + \frac{a}{b}}{\sin(el) + \frac{a}{\sin(el) + \frac{b}{c}}} + \frac{dm(el)}{dh} \quad \dots (13)$$

$$\frac{dm(el)}{dh} = \frac{1}{\sin(el)} - f(\epsilon, a_{ht}, b_{ht}, c_{ht}) \quad \dots (14)$$

$$m_{wt}(el) = \frac{1 + \frac{a_{wt}}{b_{wt}}}{\sin(el) + \frac{a_{wt}}{\sin(el) + \frac{b_{wt}}{c_{wt}}}} \quad \dots (15)$$

where el is the elevation angle. $f(\epsilon, a_{ht}, b_{ht}, c_{ht})$ is the three-term continued fraction, a_{ht} , b_{ht} and c_{ht} are the height correction coefficients.

Since in the present study, our objective is to determine wet delay using IRNSS data, the total tropospheric delay (T) given in Eq. (2) is divided into its hydrostatic and wet delay components as shown in Eq. (11) where ZWD is unknown variable. The pressure values obtained from NCEP are used to derive the zenith hydrostatic delay (ZHD) which remains almost constant for every iteration as there is not much change in atmospheric pressure during the day while the ZWD starting with the initial value is updated after every iteration considering all measurements. Other components of Eq. (2) are also retrieved from processed datasets for every iteration. So at the end of process, an updated ZWD will be retrieved which is further used for PWV estimation.

2.3 Precipitable water vapour (PWV)

The precipitable water vapour is estimated using following relation

$$PWV = \Pi * ZWD \quad \dots (16)$$

where Π is defined as

$$\Pi = \frac{10^6 * M_w}{\rho R (k_2 - k_1 \frac{M_w}{M_d} + \frac{k_3}{T_m})} \quad \dots (17)$$

where ρ is the density of liquid water, T_m is weighted mean temperature of troposphere ($T_m = 0.75T_s + 62.6$). Here T_s is the surface temperature²⁶. R , k_1 , k_2 , k_3 , M_w , M_d are the constants. $K_1 = 77.69 \text{ Khpa}^{-1}$, $K_2 = 71.2952 \text{ Khpa}^{-1}$ and $K_3 = 3.776 * 10^5 \text{ K}^2\text{hpa}^{-1}$

To get the reference values, GPS datasets are processed using GAMIT software and, obtained tropospheric delay is used for wet delay estimation. This wet delay is further used for PWV estimation using the Eqs (16) and (17). A GPS receiver is installed in the same campus to obtain the GPS data. MERRA PWV is downloaded from GIOVAANI portal over the location for the validation²⁵.

3 Results and Discussion

Precipitable water vapour is an important component of the atmosphere. Its precise value is required for various applications like weather forecasting, now casting, rainfall prediction etc. GNSS provides continuous measurement of PWV in all weather conditions. In this work, an attempt is made to develop a methodology to derive the PWV using IRNSS datasets.

From Fig. 2, it can be observed that there are three geostationary and 4 geosynchronous satellites. The geosynchronous satellite orbits in such a way that a

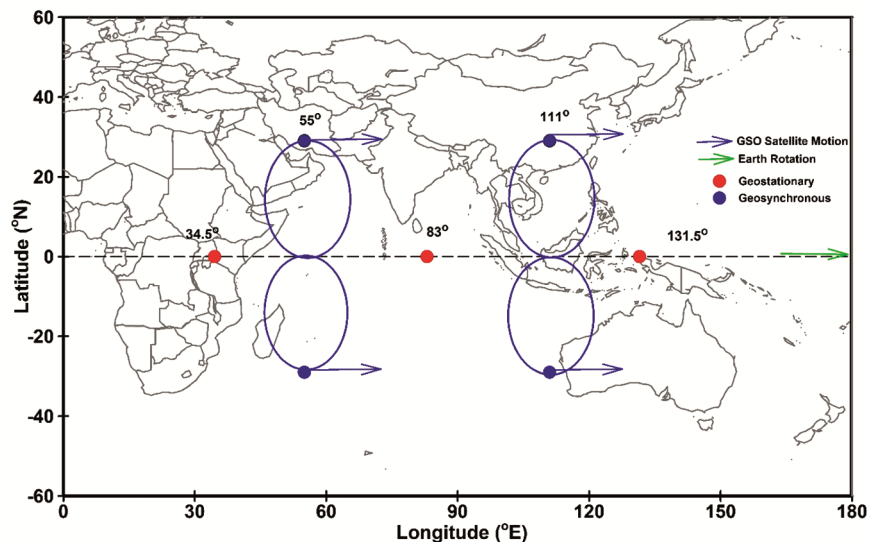


Fig. 2 — IRNSS (NavIC) constellation

minimum of 4 satellites from this constellation are always visible to a receiver over the Indian region. However, their movement is limited over a spatial map and it transmits signals continuously to the receiver without any gap. The advantage of the geo-based constellation is the all-time availability of signals from a single source for a particular region. However, in this case, signals are restricted to transmit from one direction. So, it can provide precise information on atmospheric parameters in that direction or it may have more impact from one direction while deriving the atmospheric parameter. On the other side, the low and medium earth orbit constellation transmits the signal continuously using

more satellites that rise and set from the local horizon. The advantage, in this case, is that the signal comes to the receiver from all directions at different elevation angles, which provides the information of the surrounding atmosphere. This is essential while deriving the atmosphere information from these signals. Here, since the satellites rise or set from the local horizon, a different combination of satellites is visible to the receiver over some time. So, to derive the atmospheric parameters from these satellites, the biases, and errors of each satellite should be precisely known.

Figure 3 shows that PRN2, PRN4, and, PRN5 are the geosynchronous satellites and, PRN3, PRN6 and,

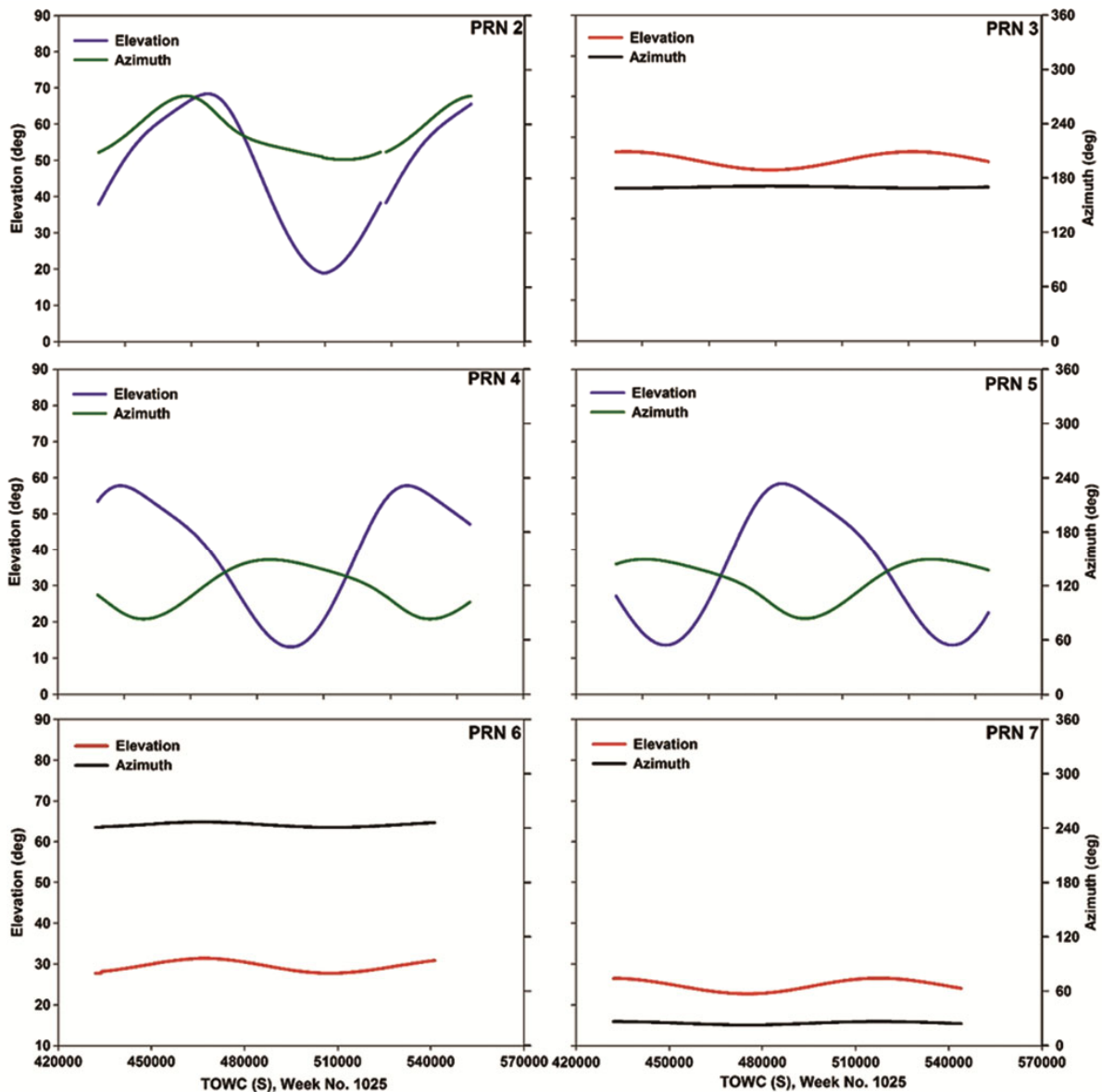


Fig. 3 — Azimuth and Elevation pattern of IRNSS satellites over Dehradun

PRN7 are the geostationary satellites. PRN2 elevation varies from 20° to 70° while for PRN4 and PRN5 the elevation varies between 10° to 60° . This reflects that, though the zenith signals are not available still sufficient level of angular height is covered. In the case of azimuth variation of these satellites, PRN2 signals are available within 210° to 270° and around 120° with less variation for PRN4 and PRN5 shows that the signals are available from a very small segment of azimuth. The azimuth and elevation graphs of PRN3, PRN6, and PRN7 show an almost linear pattern. This means that the receiver receives

signals from one direction at almost constant elevation and azimuth angles. Fig. 4 shows the movement of satellites in terms of Cartesian coordinates. It can be seen that very little change in the X and Y components, while only the Y component changes significantly for PRN2, PRN4, and PRN5. For PRN3, PRN6, and PRN7 there is almost no significant change in the coordinates. The figure also explains the pseudo-ranges which also show a similar pattern. The less variation in numbers plays an important role while estimating PWV. This way data from different directions will not be

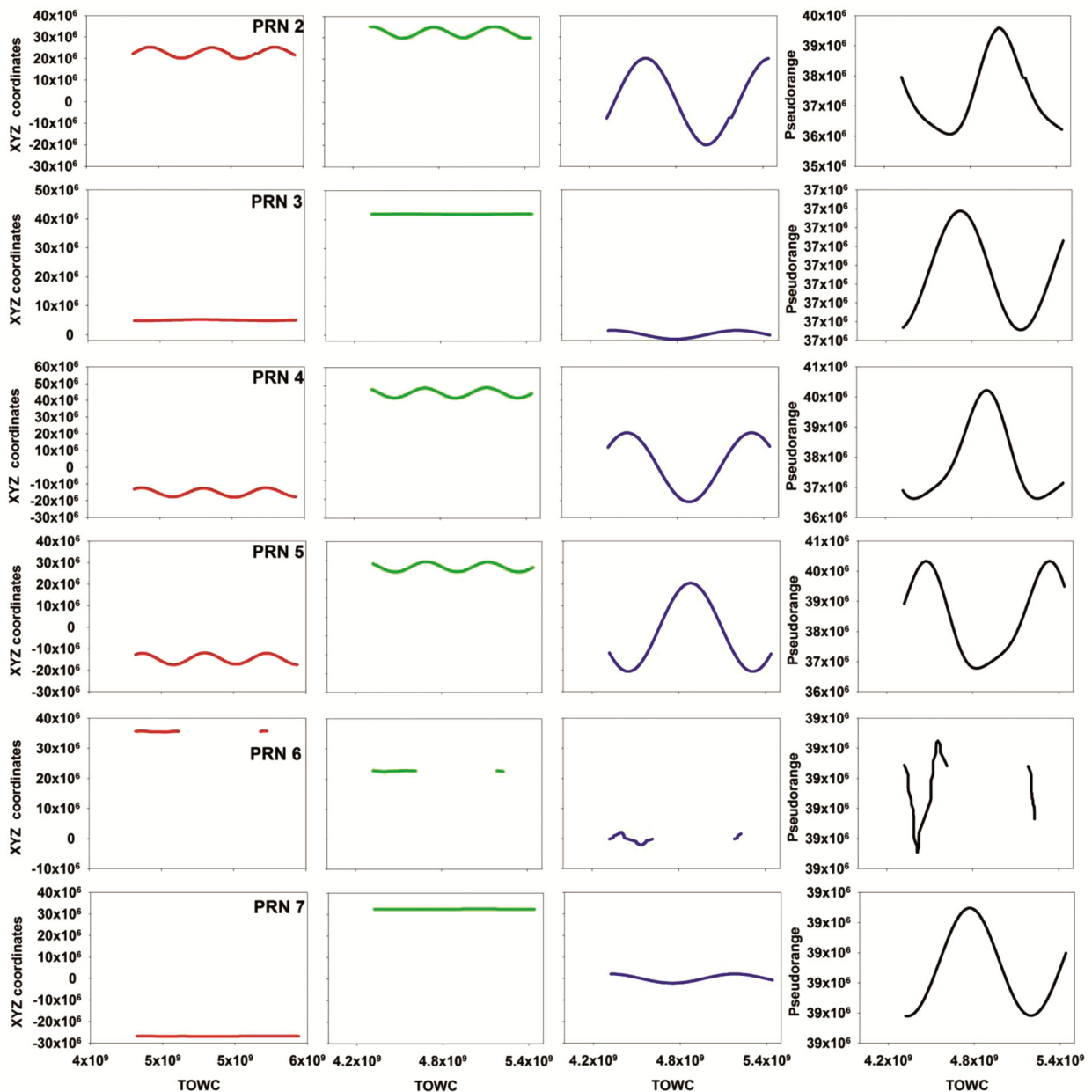


Fig. 4 — X, Y, Z (ECEF) and Pseudo range variation of IRNSS satellites over Dehradun

obtained. However, modeling of error in one direction can be easy and does not have much variation. PRN1 data are not available continuously so not taken in the study.

PWV is estimated for the months of January, April, July, and November and is represented in Figs. 5-8 respectively. Different months are selected to estimate the PWV for different sessions to validate the methodology while comparing with PWV derived from other sources and to observe the PWV variation. Since limited data are available for these months, 4 representative days are selected of which data are available for a complete day from these months. In Fig. 5, the estimated PWV is shown for day no. 24, 25, 26 and 28. This estimated PWV is compared with Modern-Era Retrospective Analysis for Research and Application (MERRA) PWV and GPS-derived PWV values. From the figure, it is seen that the estimated PWV using individual IRNSS satellite data is near to

the reference values for all days. The difference between IRNSS-derived PWV and MERRA PWV varies between 3 to 5 mm. However, in the case of combined PWV, it is closer to MERRA PWV in most of the cases having differences within 5 mm. Similarly, if compared with GPS-derived PWV it also has a difference of nearly 3 to 5 mm. Fig. 6, which represents the PWV for April month shows a PWV difference of approximately 10 mm if PRN2, PRN4, and PRN5 data are used for day no. 107 while it is close to the reference PWV for day no. 110. This may also depend on particular day data quality. On other days, results of individual satellite-derived PWV also closely match with reference values. However, in the case of combined PWV that shows within 3 mm difference from reference values, is a good estimation of IRNSS PWV. A similar phenomenon also was seen for the monsoon session, where PWV estimated results are close to the reference results and have a

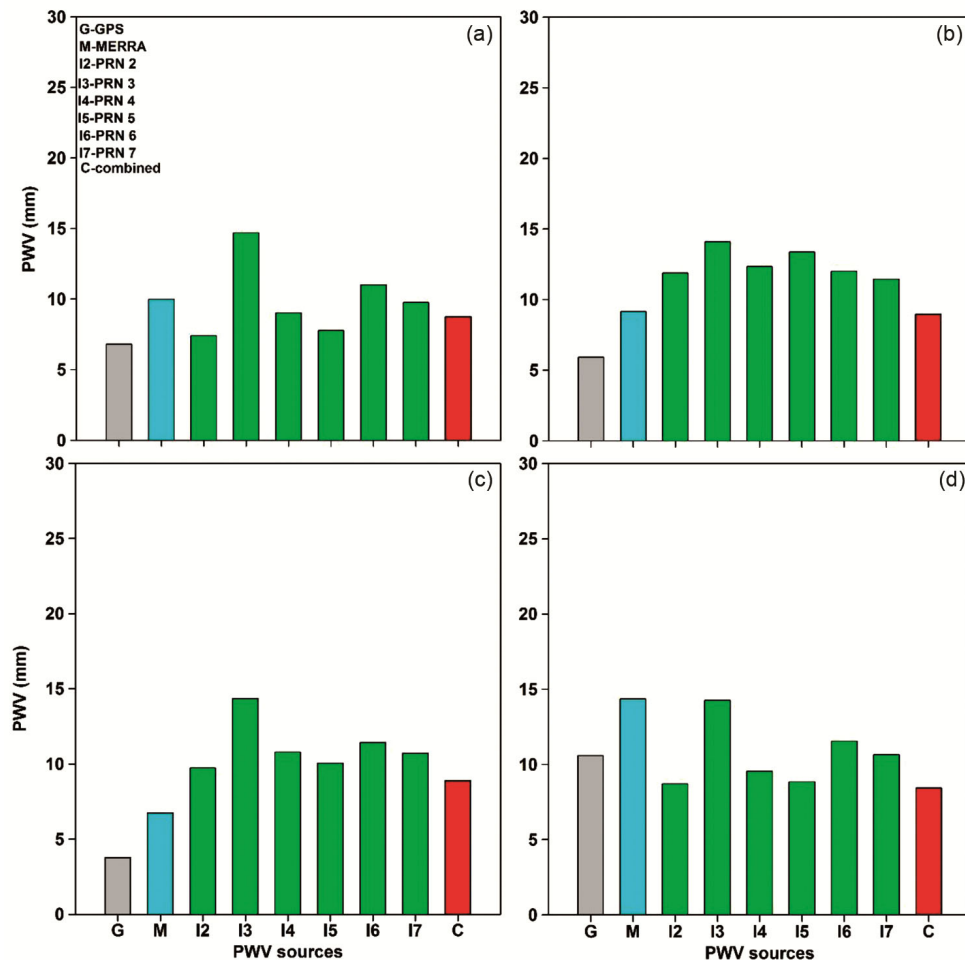


Fig. 5 — PWV variation for day number (a) 25 (b) 27 (c) 29 and (d) 30 in January 2019

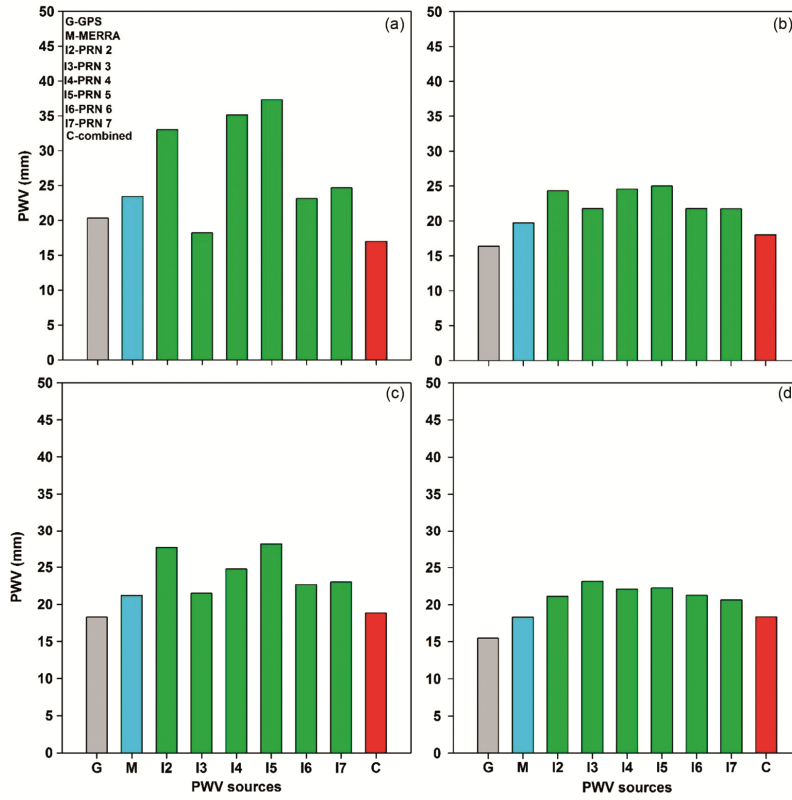


Fig. 6 — PWV variation for day number (a) 107 (b) 109 (c) 110 and (d) 111 in April 2019

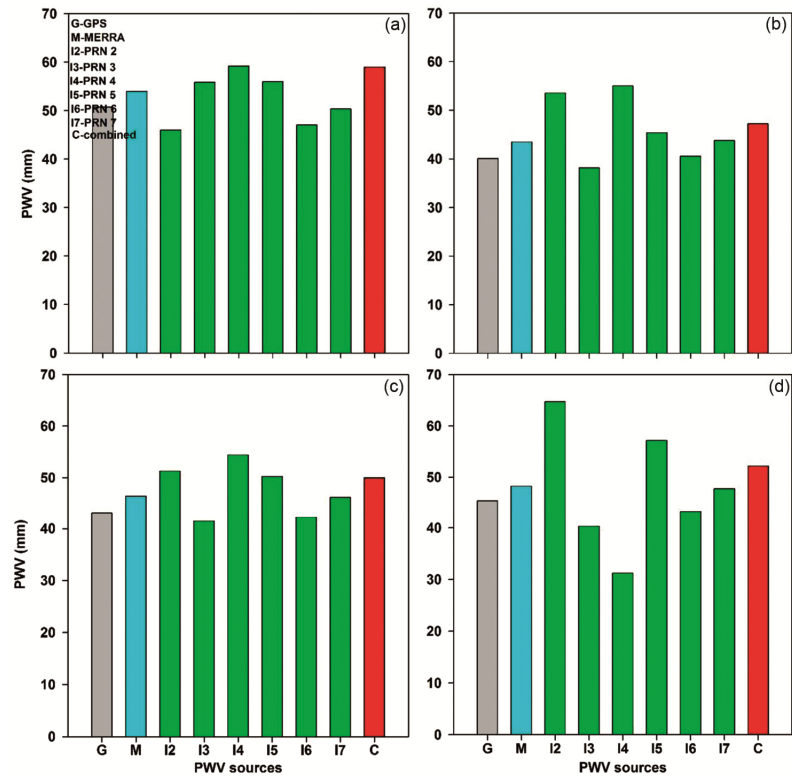


Fig. 7 — PWV variation for day number (a) 190 (b) 194 (c) 195 and (d) 196 in July 2019

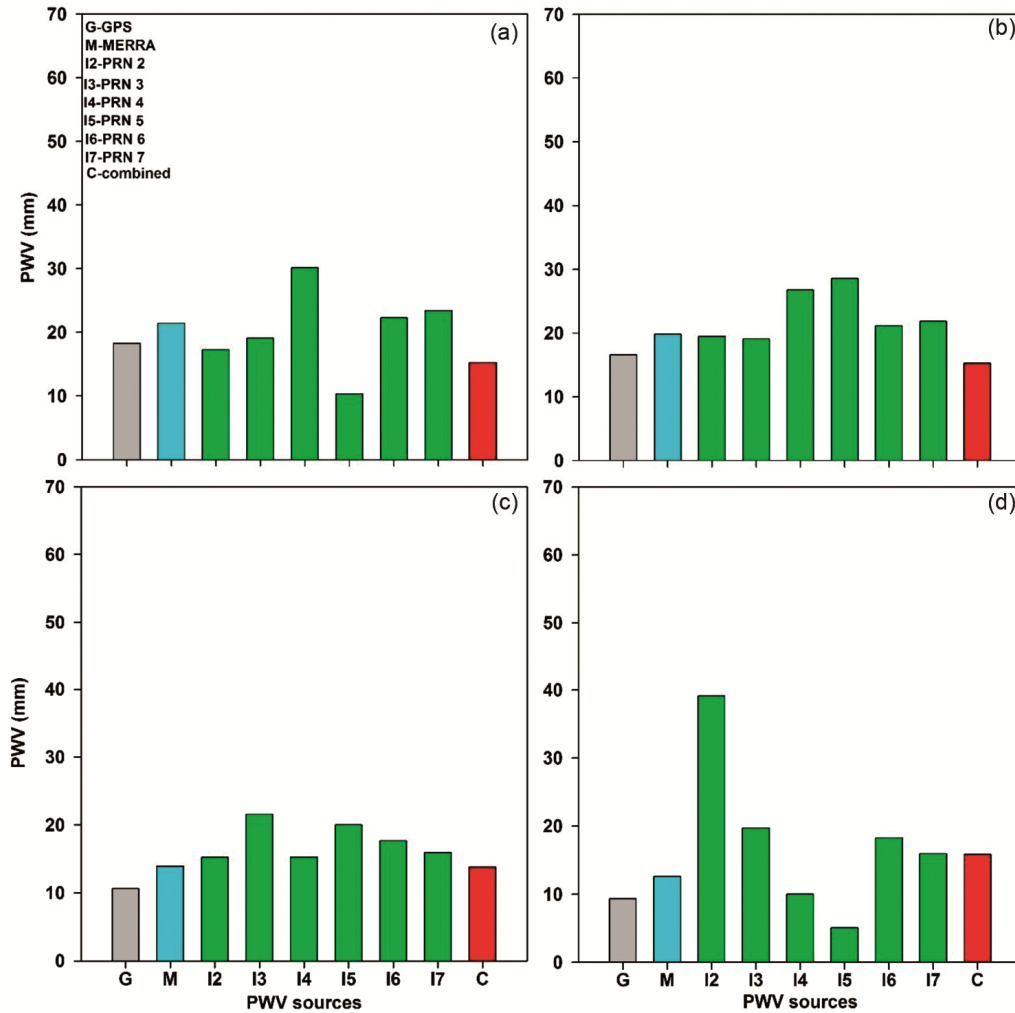


Fig. 8 — PWV variation for day number (a) 306 (b) 307 (c) 308 and (d) 309 in November 2019

difference if combined data are used while it varies in case individual satellite data are used. The results are also close to the GPS-derived PWV. In the monsoon session, higher values of PWV are expected, as can be seen from Fig. 7 due to more water vapour present in the atmosphere. From the figure, it is also clear that using a developed algorithm for IRNSS data, it can be captured very effectively. However, convergence needs more iterations in some of these cases. The PWV was derived using combined data 3 to 4 mm difference from reference results. Fig. 8 represents the estimated PWV results for the month of November, which are after the monsoon session, and less PWV is expected in this case. For all the days a close observation of PWV with MERRA PWV was observed using IRNSS data. Combined PWV values have differences within 4-5 mm with reference values.

Figures 9-11 represent the statistical relation between IRNSS PWV with GPS and MERRA PWV. From Fig. 9, a good correlation can be observed between IRNSS PWV and MERRA PWV. In the case of PRN2, PRN4, and PRN5 the R^2 value is less compared to PRN3, PRN6, and PRN7. However, this also shows a good correlation. Fig. 10 shows a good correlation between GPS PWV and IRNSS PWV. Here, also IRNSS PWV retrieved from geostationary satellites correlates strongly with GPS PWV. Fig. 11 shows a correlation between IRNSS PWV using combined data and GPS and MERRA PWV, which also holds a strong correlation. From this analysis, it can be stated that a good estimation of PWV can be obtained using individual IRNSS satellite data using a developed algorithm. Using the combined data from the satellites, the estimated PWV shows a strong correlation with reference results.

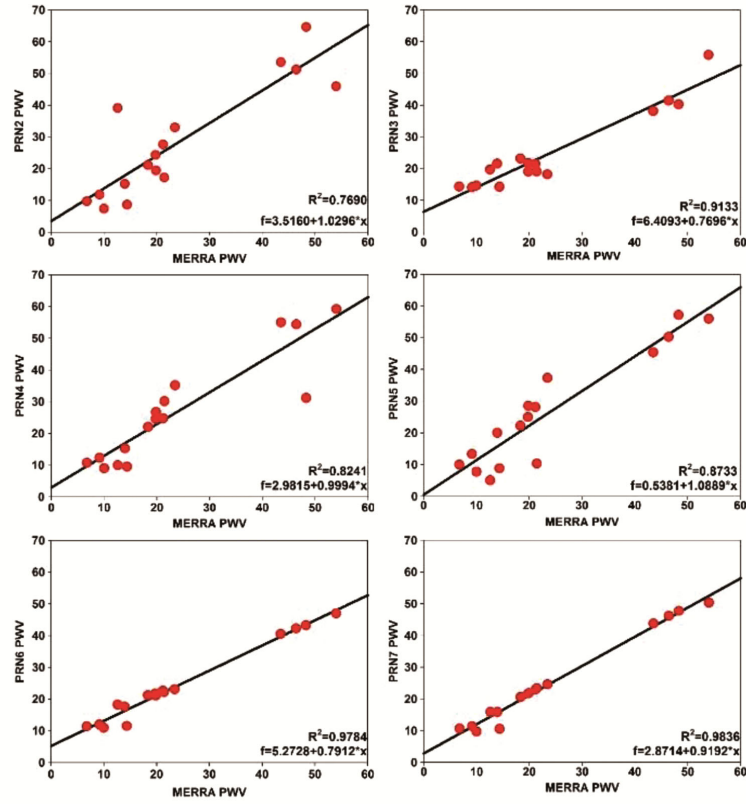


Fig. 9 — Regression analysis between IRNSS derived PWV and MERRA PWV

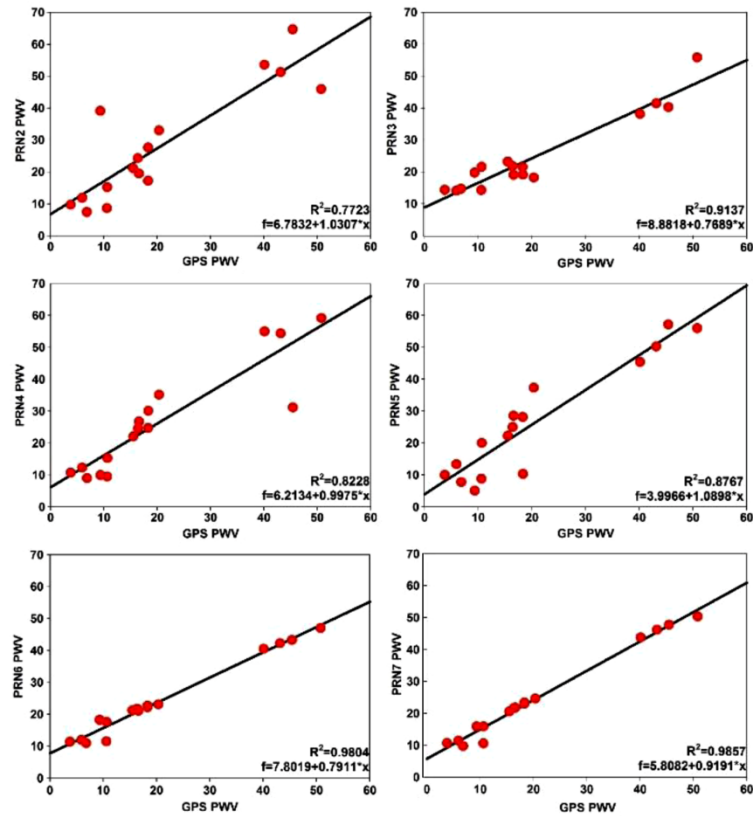


Fig. 10 — Regression analysis between IRNSS and GPS derived PWV

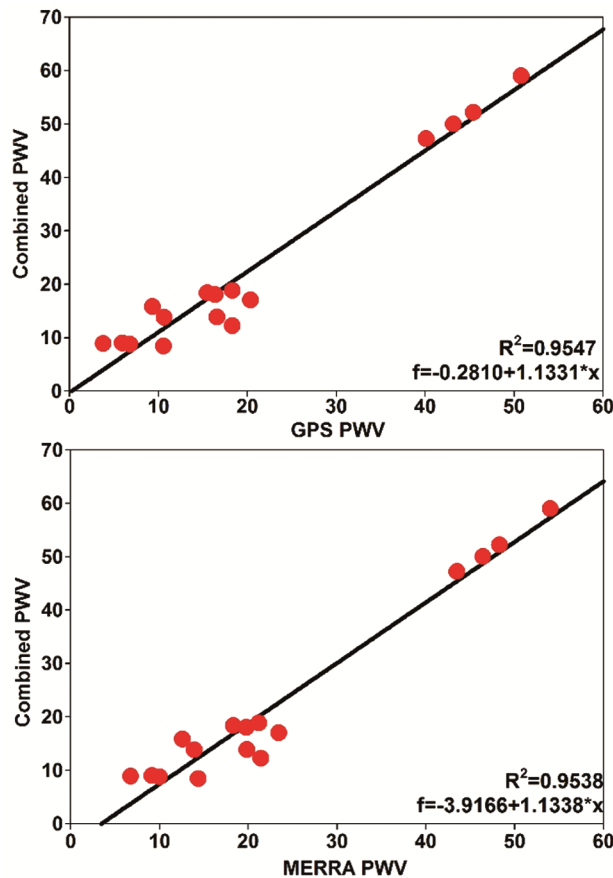


Fig. 11 — Regression analysis between IRNSS derived PWV (Combined) with GPS and MERRA PWV

4 Conclusion

In recent times navigation signals have been used to derive atmospheric parameters apart from its regular application of position estimation. GPS-derived precipitable water vapour is an example of such an application and is used in weather forecasting and atmospheric applications. On the other side, India has developed its regional navigation system, of which signals are available at all times over the Indian region and used for precise positioning. In this work, the first time an attempt is made to derive the precipitable water vapour using IRNSS data. To obtain IRNSS data, an IRNSS receiver is set up at the top of a building at IIRS, Dehradun, which provides data at regular intervals. Since each satellite's signals are available at all time over the region, PWV is estimated using individual satellite data separately and combined data from all the satellites. An algorithm is developed to estimate PWV using IRNSS data. The differential correction least square technique is applied to derive the zenith tropospheric delay (ZTD). Zenith wet delay (ZWD) is obtained after

subtracting the zenith hydrostatic delay (ZHD) which is estimated using NCEP global reanalysis data. Further, ZWD is used to estimate PWV by multiplying a constant. Estimated PWV values are compared with the MERRA PWV values taken from the GIOVANNI and GPS-derived PWV values. The obtained results show good agreement with MERRA and GPS PWV values. This study shows that by using IRNSS data also a good estimation of PWV can be obtained. However, it depends on data quality, initial guess, convergence criteria, etc. and is subject to further improvement.

Acknowledgements

The authors would like to thank to Dr. Vandita Srivastava, Head Geoinformatics Department, Smt. Shefali Agrawal, Group Head GTOGP, and Dr. R. P. Singh Director, IIRS for their encouragement and support. The authors are grateful to the data provider team of NCEP, and GIOVANNI. We thank anonymous reviewers, editors for their critical comments and suggestions which made us improve this manuscript significantly.

Conflict of interest

The author declare that there is no conflict of interest.

References

- 1 Bevis M, Businger S, Herring T A, Rocken C, Anthes R A & Ware R H, *J Geophys Res: Atmos*, 97 (1992) 15787.
- 2 Niell A E, *J Geophys Res: Sol Earth*, 101 (1996) 3227.
- 3 Dai A, Wang J, Ware R H & Van Hove T, *J Geophys Res: Atmos*, 107 (2020) ACL-11.
- 4 Wang J, Zhang L, Dai A, Van Hove T & Van B J, *J Geophys Res: Atmos*, 112 (2007).
- 5 Jade S & Vijayan M S M, *J Geophys Res: Atmos*, 113 (2008).
- 6 Adams D K, Fernandes R M, Bennett R A, Spinler J C, Chagas G, Tanaka L M & Cirino G, *AGUFM*, A53 (2012) S-05.
- 7 Bonafoni S, Mazzoni A, Cimini D, Montopoli M, Pierdicca N, Basili P & Carlesimo, *GPS Solutions*, 17 (2013) 475.
- 8 Joshi S, Kumar K, Pande B & Pant M C, *Meteorol Atmos Phys*, 120 (2013) 177.
- 9 Shoji Y, Yamauchi H, Mashiko W & Sato E, *Sola*, 10 (2014) 29.
- 10 Arboledas L, *J Geophys Res: Atmos*, 119 (2014) 9596.
- 11 Singh D, Ghosh J K & Kashyap D, *Meteorol Atmos Phys*, 123 (2014) 209.
- 12 Alshawaf F, Fuhrmann T, Knöpfler A, Luo X, Mayer M, Hinz S & Heck B, *IEEE Trans Geosci Remote Sens*, 53 (2015) 3764.
- 13 Liang H, Cao Y, Wan X, Xu Z, Wang H & Hu H, *Geodesy Geodynamics*, 6 (2015) 135.
- 14 Lu C, Li X, Nilsson T, Ning T, Heinkelmann R, Ge M & Schuh H, *J Geodesy*, 89 (2015) 843.

- 15 Jiang P, Ye S, Chen D, Liu Y & Xia P, *Remote Sens*, 8 (2016) 389.
- 16 Isiye O A, Ludwig C & Joel O B, *Int J Remote Sens*, 38 (2017) 5710.
- 17 Kitpracha C, Promchot D, Srestasathiern P & Satirapod C, *Int J Geoinformat*, 13 (2017) 17.
- 18 Hankansurijat C & Andrei O, *Eng J*, 22 (2018) 37.
- 19 Yao Y, Xu X & Hu Y, *Atmos MeasTech Discuss*, 1 (2018).
- 20 Zhang Q, Ye J, Zhang S & Han F, *J Sens*, (2018).
- 21 Liu C, Zheng N, Zhang K & Liu J, *J Sens*, 19 (2019) 698.
- 22 Meunram P & Satirapod C, *Geodesy Geodynamics*, 10 (2019) 140.
- 23 Darrag M, AbouAly N, Mohamed A M S, Becker M & Saleh M, *Acta Geodaetica et Geophysica*, (2020) 1.
- 24 Mruthyunjaya L & Ramasubramanian R, URL < <https://www.isro.gov.in/irnssprogramme>. (2017).
- 25 Gelaro R, McCarty W, Suárez M J, Todling R, Molod A, Takacs L & Zhao B, *J Climate*, 30 (2017) 5419.
- 26 Raju C S, Saha K, Thampi B V & Parameswaran K, *Annal Geophys Atmos Hydros Space Sci*, 25 (2007) 1935.